JACS
JOURNAL OF THE AMERICAN CHEMICAL SOCIETY
Article
pubs.acs.org/JACS

Adsorption of Small Organic Molecules on Graphene

Petr Lazar,‡ František Karlický,‡ Petr Jurečka, Mikuláš Kocman, Eva Otyepková, Klára Šafářová, and Michal Otyepka*

Regional Centre of Advanced Technologies and Materials, Department of Physical Chemistry, Faculty of Science, Palacký University Olomouc, 771 46 Olomouc, Czech Republic

Supporting Information

ABSTRACT: We present a combined experimental and theoretical quantification of the adsorption enthalpies of seven organic molecules (acetone, acetonitrile, dichloromethane, ethanol, ethyl acetate, hexane, and toluene) on graphene. Adsorption enthalpies were measured by inverse gas chromatography and ranged from −5.9 kcal/mol for dichloromethane to −13.5 kcal/mol for toluene. The strength of interaction between graphene and the organic molecules was estimated by density functional theory (PBE, B97D, M06-2X, and optB88-vdW), wave function theory (MP2, SCS(MI)-MP2, MP2.5, MP2.X, and CCSD(T)), and empirical calculations (OPLS-AA) using two graphene models: coronene and infinite graphene. Symmetry-adapted perturbation theory calculations indicated that the interactions were governed by London dispersive forces (amounting to ∼60% of attractive interactions), even for the polar molecules. The results also showed that the adsorption enthalpies were largely controlled by the interaction energy. Adsorption enthalpies obtained from *ab initio* molecular dynamics employing non-local optB88-vdW functional were in excellent agreement with the experimental data, indicating that the functional can cover physical phenomena behind adsorption of organic molecules on graphene sufficiently well.

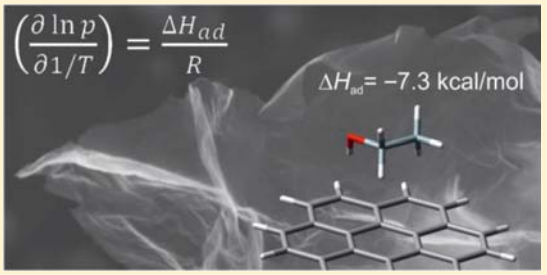

INTRODUCTION

Since its discovery, graphene[1] has been demonstrated to have promising applications in diverse disciplines, ranging from electronics to medicine.[2,3] It has been shown that the potential applications of graphene can be extensively broadened by various modes of functionalization, including non-covalent binding (adsorption) of molecules and nanoparticles.[4] One particularly interesting branch of research is the development of graphene-based chemical detectors, which can achieve such a high level of sensitivity that individual molecules adsorbed on graphene can be detected.[5,6] However, further progress requires quantification and understanding of the interaction of adsorbed molecules with graphene.

Quantification and identification of the nature of the interaction of adsorbed molecules on graphene pose several challenges from a theoretical perspective. Adsorption of small single molecules on graphene can be evaluated by quantum mechanical calculations based on density functional theory (DFT).[7,8] DFT can readily accommodate the periodic boundary conditions necessary to model a graphene sheet and can, in principle, calculate the adsorption properties of an arbitrary molecule. However, the reliability of the results obtained with the most widely used exchange-correlation DFT functionals, i.e., local density approximation (LDA) and generalized gradient approximation (GGA),[9,10] is often inadequate. In particular, omission of non-local electron correlations can severely affect the calculated adsorption properties because the interaction of guest molecules with graphene involves a large component of London dispersive forces of non-local nature. Recently, several techniques have been developed to combat this shortcoming, ranging from empirical corrections[11] and addition of a non-local correlation core (vdW-DF)[12] up to fully non-local and computationally expensive methods, such as random phase approximation.[13,14] However, there is a current lack of suitable experimental data with which to assess the performance of these methods.

In this paper, we present a combined experimental and theoretical study of the adsorption of seven small organic molecules onto graphene, which aimed to identify the magnitude and nature of the interaction. We used inverse gas chromatography to determine the adsorption enthalpies of gas-phase molecules to graphene flakes. This method allows adsorption enthalpies of volatile organic compounds onto a given surface to be measured directly and has previously been used to determine surface and interaction properties of various carbon-based materials, e.g., graphite,[15,16] carbon nanotubes,[17] and activated carbon.[18] However, to date, no reports have analyzed the interaction of molecules with graphene. To address this deficiency, we performed *ab initio* molecular dynamics (AIMD) simulations based on DFT to identify energetically favorable configurations of adsorbed molecules and evaluate the adsorption energies. In particular, we investigated use of the optB88-vdW DFT functional, which includes a contribution from non-local correlations.[19] For comparison, we also evaluated the adsorption properties using

Received: March 29, 2013
Published: April 9, 2013

dx.doi.org/10.1021/ja403162r | J. Am. Chem. Soc. 2013, 135, 6372−6377

an empirical force field typically used to analyze the interaction of graphene with large assemblies, such as nucleobases[20,21] or large molecules.[22,23] In addition, we calculated the properties of molecules adsorbed on coronene, which has been suggested to be a suitable small model of graphene.[24−28] The coronene model also allows the treatment of non-local correlations via the benchmark CCSD(T) method and evaluation of the contributions to the enthalpy of adsorption arising from zero-point and thermal vibrations. The nature of the interaction was examined in further detail using the symmetry-adapted perturbation theory (SAPT) method.[29]

EXPERIMENTAL AND COMPUTATIONAL METHODS

Differential isosteric adsorption enthalpies (heats of adsorption), ΔH_{ads}, were measured by inverse gas chromatography (iGC) using an SMS-iGC 2000 instrument (Surface Measurement Systems, UK) equipped with an SMS silylated column (diameter 4 mm, length 30 cm) containing 18.8 mg of graphene flakes (Graphenesupermarket, AO-1) with a surface area of 510 m^2/g. Measurements were carried out with *n*-hexane (Merck, LiChrosolv for LC, ≥98%), toluene (Sigma-Aldrich, Chromasolv for HPLC, 99.9%), dichloromethane (Merck, LiChrosolv for LC, ≥99.9%), ethyl acetate (Lach:ner, for HPLC, min. 99.8%), ethanol (Merck, gradient grade LiChrosolv for LC, ≥99.9%), and acetonitrile (Lach:ner, HPLC supergradient, min. 99.9%).

The adsorption enthalpies ΔH_{ads} for a given coverage ν can be calculated from the Clausius−Clapeyron equation:

$$\left(\frac{\partial P}{\partial T}\right)_{\nu} = \frac{\Delta H_{ad}}{T\Delta V} \tag{1}$$

where T is the thermodynamic temperature. Assuming ideal gas behavior and that ΔV is approximately equal to the volume of vapor in the gas phase, this equation can be rewritten as

$$\left(\frac{\partial \ln P}{\partial\, 1/T}\right)_{\nu} = \frac{\Delta H_{ad}}{R} \tag{2}$$

where R is the universal gas constant and P is pressure. The adsorption enthalpy can then be derived from a plot of $\ln P$ vs $1/T$. Further details on how $\ln P$ can be calculated from elution times measured by iGC can be found in the literature.[30,31]

Scanning electron microscopy (SEM) images were captured on a Hitachi 6600 FEG microscope operating in the secondary electron mode and using an accelerating voltage of 5 kV. Energy dispersive X-ray spectra (EDS) were also captured on this microscope by using a NORAN System 7 X-ray microanalysis system and an accelerating voltage of 5 kV. The SEM sample comprised a dried powder sample mounted on an aluminum holder with double-sided adhesive carbon tape.

Benchmark wave function calculations were performed for model complexes on coronene using the TurboMole 6.3 program[32] and Molpro 2012 package.[33] The CCSD(T)/CBS estimate was obtained by extrapolating[34] the cc-pV(T,Q)Z/MP2 energies and correcting for higher order correlation effects obtained at the CCSD(T)/cc-pVDZ level.[35] MP2.5/CBS and MP2.X/CBS energies were evaluated analogically, with the correction term obtained at the MP3/cc-pVDZ level.[36] The SCS(MI)-MP2 method was used with parameters of c_{OS} = 0.4 and c_{SS} = 1.29, as recommended for cc-pV(T,Q)Z extrapolation.[37] All energies were corrected for the basis set superposition error by using the counterpoise correction[38] (see Supporting Information for rigorous definitions and details). Geometry optimizations were carried out with cc-pVDZ and cc-pVTZ basis sets for MP2 and M06-2X,[39] and B97D,[40] respectively, using the Gaussian09 package.[41] Frequency calculations were performed at the B97D/cc-pVTZ level to determine the zero-point energy ($\Delta\Delta E_0$), thermal ($\Delta\Delta E_T$), and enthalpy ($\Delta\Delta E_H$) corrections. These corrections contribute to the enthalpy ΔH and internal energy ΔU as follows:

$$\Delta H = \Delta E + \Delta\Delta E_0 + \Delta\Delta E_T + \Delta\Delta E_H \tag{3}$$

$$\Delta U = \Delta E + \Delta\Delta E_0 + \Delta\Delta E_T$$

where ΔE stands for the electronic energy. All electronic energies discussed in the text are *adsorption* (i.e., *stabilization*) *energies*, ΔE, defined as the energy difference between the complex and infinitely separated fragments (graphene/coronene and molecule), whereas the *interaction energy*, ΔE_{int}, corresponds to fragments with the geometry of the complex. The difference between the adsorption and interaction energies is termed the *deformation energy*, E_{def}, of the fragments, i.e., $\Delta E = \Delta E_{int} + E_{def}^{gr} + E_{def}^{mol}$ (see Supporting Information for further details).

SAPT decomposition allows the interaction energy to be partitioned into physically meaningful components. Here, we used DFT-SAPT[42−45] implemented in the Molpro program package.[33] The components obtained from the SAPT calculation were gathered into four terms corresponding to electrostatics, exchange repulsion, induction, and dispersion:

$$E^{SAPT} = E_{elst} + E_{exch\text{-}rep} + E_{ind} + E_{disp} \tag{4}$$

where E_{elst} is $E_{elst}^{(1)}$, $E_{exch\text{-}rep}$ is $E_{exch\text{-}rep}^{(1)}$, E_{ind} is $E_{ind}^{(2)} + E_{exch\text{-}ind}^{(2)} + \delta(\mathrm{HF})$, and E_{disp} is $E_{disp}^{(2)} + E_{exch\text{-}disp}^{(2)}$ (for more details on DFT-SAPT, see the references above). We used the LPBE0AC exchange-correlation potential[42−49] for monomer calculations and a cc-pVTZ basis set.

DFT calculations on graphene were performed using the projector-augmented wave (PAW) method in the Vienna Ab initio Simulation Package (VASP) suite.[50,51] The energy cutoff for the plane-wave (PW) expansion was set to 400 eV, as further increasing the energy cutoff to 500 eV resulted in no change in the calculated adsorption energies. The graphene sheet was modeled using a 4×4 supercell (32 carbon atoms) with a calculated C−C bond length of 1.44 Å. The periodically repeated sheets were separated by 15 Å of vacuum. The AIMD simulation was used to mimic finite temperature effects; molecules were placed onto a graphene sheet, and the system was treated as a canonical (NVT) ensemble. The temperature in the simulation was set to 333 K, which was typical of the temperature used in the experiment. AIMD simulations were performed for at least 5 ps with a time step of 1 fs. Adsorption energies were obtained by quenching low-energy configurations from the AIMD run (ΔE^{AIMD}) and by time-averaging Kohn−Sham energies $\Delta\langle E^{AIMD}\rangle$ obtained in the AIMD simulation. In order to determine enthalpies of adsorption ΔH^{AIMD}, we corrected the adsorption energies on graphene, ΔE^{AIMD}, by the zero-point ($\Delta\Delta E_0$) and thermal ($\Delta\Delta E_T$) corrections from the coronene model and $-RT$ ($\sim\Delta\Delta E_H$). The $\Delta\langle E^{AIMD}\rangle$ obtained from the AIMD simulations intrinsically included thermal corrections. Thus, the respective enthalpy $\Delta\langle H^{AIMD}\rangle$ was calculated by adding zero-point energy and $-RT$ corrections only.

Force field (FF) simulations were performed using all-atom optimal potentials for liquid simulation (OPLS-AA).[52] Structures and topologies of the molecules were taken from the Gromacs Molecule & Liquid Database.[53,54] Graphene was modeled by 3936 atoms, which were kept in fixed positions in a planar hexagonal lattice with a bond distance of 1.4 Å. Periodic boundary conditions were applied in all three dimensions of the simulation box, which had a size of 100 × 100 × 130 Å. Intermolecular interactions were calculated using the Lennard-Jones potential described by Chang and Steele[55] with a cutoff radius of 10.0 Å. The Newtonian equations of motion were integrated using a 2 fs time step. Each MD run was equilibrated for 0.2 ns, and the energy $\Delta\langle E^{FF}\rangle$ of the molecule−graphene interaction was calculated as an average of 5000 values over 1 ns of simulation time. All simulations were performed with a constant volume and a temperature of 323 K. The adsorption enthalpies from force field simulations were calculated as follows:

$$\Delta\langle H^{FF}\rangle = \Delta\langle E^{FF}\rangle - RT \tag{5}$$

where $-RT$ corresponds to the enthalpy correction ($\Delta\Delta E_H$).

dx.doi.org/10.1021/ja403162r | J. Am. Chem. Soc. 2013, 135, 6372−6377

RESULTS AND DISCUSSION

Experiment. The adsorption enthalpies (ΔH_{ads}) of the organic molecules to graphene flakes (Figure S1) measured by iGC ranged from −5.9 to −13.5 kcal/mol (Table 1).

Table 1. Experimental Adsorption Enthalpies (in kcal/mol) and Their Respective Confidence Intervals (at α = 0.05) for Seven Molecules, Measured by Inverse Gas Chromatography in the Specified Temperature Ranges (T_{min}−T_{max} in K)

compound	ΔH_{ads}	T_{min}−T_{max}
acetone	−8.2 ± 0.3	303−333
acetonitrile	−7.6 ± 0.3	303−343
dichloromethane	−5.9 ± 0.5	303−343
ethanol	−7.3 ± 0.7	303−343
ethyl acetate	−11.5 ± 0.2	303−343
hexane	−12.2 ± 0.2	333−373
toluene	−13.5 ± 0.3	343−383

Dichloromethane had the lowest ΔH_{ads}, followed by ethanol, acetonitrile, acetone, ethyl acetate, hexane, and last toluene, which displayed the highest affinity to graphene. Each measurement was conducted at five (four for acetone) temperatures (Table 1) at low coverage ν (∼2.0%), and plots of $\ln P$ against $1/T$ (Figures S2−S8) were linear for each molecule with a coefficient of determination (r^2) above 0.99, except for ethanol ($r^2 \approx 0.98$).

The same ΔH_{ads} values were obtained in consecutive independent measurements under constant conditions, confirming the reproducibility of the results. The estimated experimental error in the adsorption enthalpies was, on average, less than 0.4 kcal/mol (Table 1). The values of ΔH_{ads} depended on coverage (see Figure 1 for ΔH_{ads} of

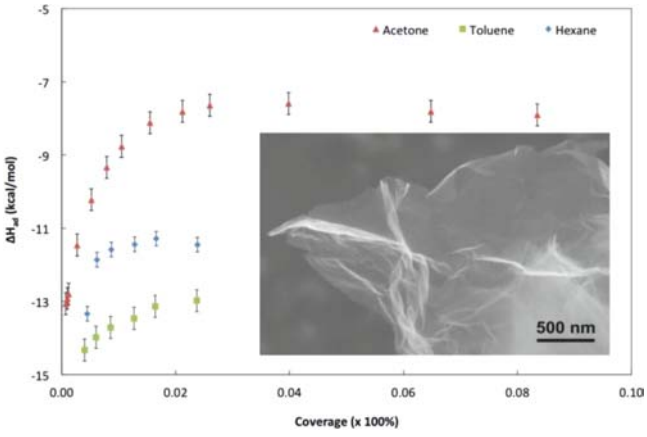

Figure 1. Adsorption enthalpies (ΔH_{ads}) of acetone, toluene, and hexane on graphene flakes vs coverage, showing saturation at ∼2% coverage. Inset: SEM image of the graphene flake.

acetone, toluene, and hexane). ΔH_{ads} was more negative at very low coverage, indicating that adsorption initially occurred onto high surface energy sites (e.g., sides and edges) of the graphene flakes but increased with increasing coverage. Once the high surface energy positions were filled, molecules then adsorbed onto the graphene surface, as manifested by the constant ΔH_{ads} value. A slight deviation from this behavior was observed for ethanol: after an initial drop, ΔH_{ads} slowly increased with increasing coverage (data not shown). This can be attributed to clustering of ethanol molecules (via hydrogen bonds) on the surface, which is also reflected in the large error bars observed for ethanol (Table 1). This may also explain the deviation of the $\ln P$ vs $1/T$ plot for ethanol from linearity (albeit not statistically significant at α = 0.05). Consequently, the ΔH_{ads} value of ethanol measured at low temperatures was lower (−9.1 kcal/mol) than that at higher temperatures (−5.2 kcal/mol).

Computations on Coronene Model. In order to unravel the nature of the interaction between the studied molecules and a graphene-like support, we performed calculations on a finite model system, i.e., coronene. The calculated geometries of molecules allowed to relax and adsorb on coronene are displayed in Figure 2. The coronene model enabled

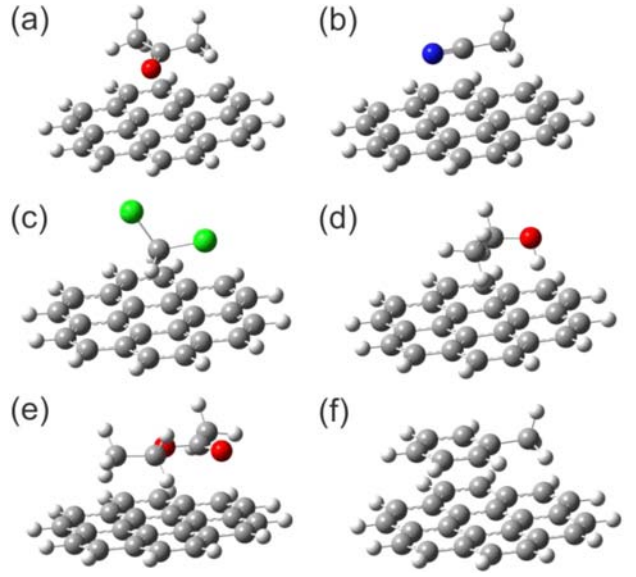

Figure 2. Calculated geometries of (a) acetone, (b) acetonitrile, (c) dichloromethane, (d) ethanol, (e) ethyl acetate, and (f) toluene adsorbed on coronene.

decomposition of the interaction energies by SAPT (Figure 3a), and computation of zero-point energy, and thermal and enthalpy corrections (Figure 3b,c), needed to convert calculated energies of adsorption into *enthalpies* of adsorption. The coronene model also enabled the strength of the interaction to be evaluated by various *ab initio* methods up to the CCSD(T) level and identification of a DFT functional suitable for the description of molecules adsorbed on graphene (Table 2, Figure 3d).

Figure 3a shows the contributions of dispersion, induction, and electrostatics calculated by SAPT to the total attractive energy. For instance, the dispersion contribution (in %) was calculated as $E_{disp}/(E_{disp} + E_{ind} + E_{elst})$. Clearly, the dispersion stabilization was dominant as it contributed more than 60% of the total attractive interaction for all the complexes considered, including those that were polar. The second largest attractive contribution was due to electrostatics, which was very large even for nonpolar molecules such as hexane. This indicates that most of the electrostatic attraction originates from large overlap (or penetration) electrostatics, which is a consequence of quite short intermolecular distances caused by strong dispersion attraction. The induction (or polarization) interaction was comparatively small in all cases. Full SAPT data are shown in Table S1.

The contributions to the enthalpy of adsorption (ΔH) according to equation 3 are displayed in Figure 3b,c. The zero-

dx.doi.org/10.1021/ja403162r | J. Am. Chem. Soc. 2013, 135, 6372−6377

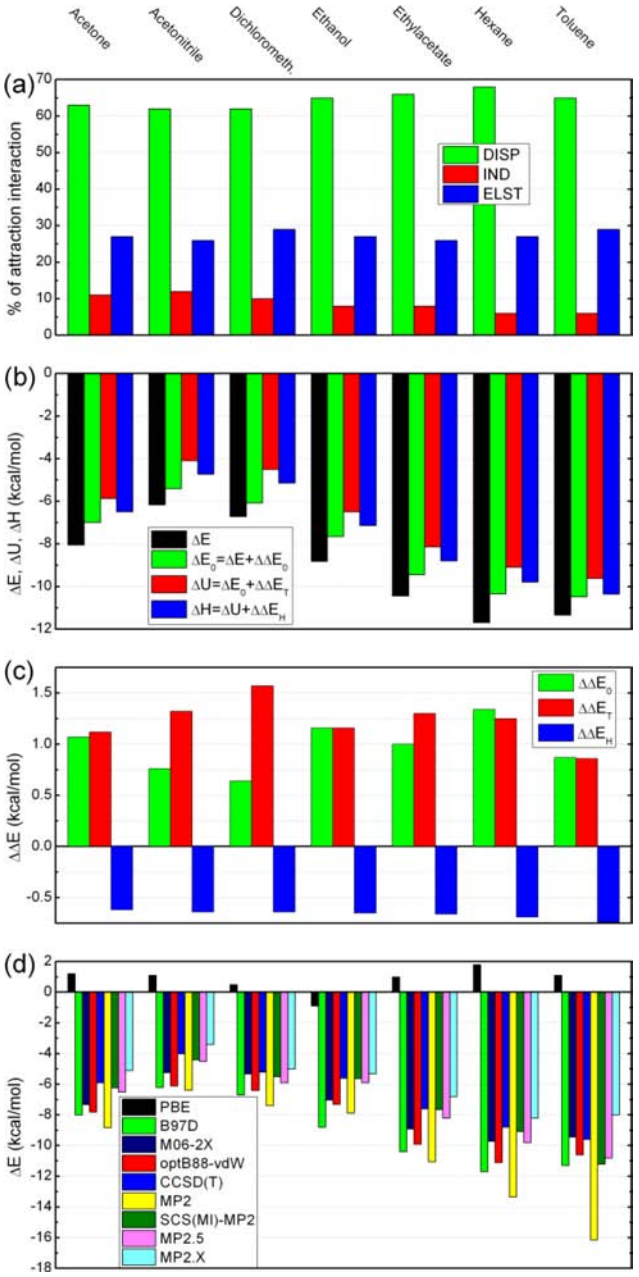

Figure 3. (a) Decomposition of the attractive contributions to the adsorption energy from SAPT. (b) Adsorption energies/enthalpies showing the contributions of the zero-point energy ($\Delta\Delta E_0$), thermal ($\Delta\Delta E_T$), and enthalpy ($\Delta\Delta E_H$) corrections. (c) Effects of the corrections to the adsorption energies. (d) Adsorption energies of the seven studied molecules on coronene calculated by various methods.

point energy corrections ($\Delta\Delta E_0$) were similar for all molecules and increased the adsorption energy by about 0.8−1.3 kcal/mol. Thermal corrections ($\Delta\Delta E_T$) further increased the final adsorption enthalpies by 0.9−1.6 kcal/mol. On the other hand, enthalpy corrections ($\Delta\Delta E_H$) had an opposite effect, decreasing the energies by ∼ −0.7 kcal/mol, i.e., by an amount similar to $-RT$ for an ideal gas. As a result, each correction had a similar magnitude for all molecules on coronene. Thus, the adsorption enthalpies (ΔH) were predominantly controlled by the adsorption energies (ΔE).

Table 2. Interaction Energies of Seven Different Molecules on Coronene (ΔE_{int} in kcal/mol) Calculated with the optB88-vdW Functional, M06-2X Functional, SCS(MI)-MP2/CBS Method, and CCSD(T)/CBS Estimate

compound	optB88-vdW/PW	M06-2X/cc-pVTZ	SCS(MI)-MP2/CBS[a]	CCSD(T)/CBS[a]
acetone	−8.5	−7.5	−7.9	−7.6
acetonitrile	−6.6	−5.4	−6.6	−6.2
dichloromethane	−6.8	−5.4	−7.0	−6.7
ethanol	−7.8	−7.1	−7.1	−7.1
ethyl acetate	−10.5	−9.1	−9.7	−9.7
hexane	−11.6	−9.9	−10.7	−10.4
toluene	−12.1	−9.7	−13.5	−11.9

[a]B97D geometries.

Figure 3d displays the calculated adsorption (stabilization) energies ΔE (obtained by adding monomer deformation energies to the interaction energies; see Methods and Supporting Information for definitions) of molecules on coronene. All methods reproduced the experimental order of adsorption energies. Compared to the CCSD(T) method, which provides the most physically robust description of dispersion interactions, the SCS(MI)-MP2, MP2.5, and MP2.X methods gave very reliable results with mean errors (MEs) of 0.4, 0.7, and 0.7 kcal/mol, respectively. However, it should be noted that the MP2 method gave consistently lower adsorption energies, reflecting the known tendency of MP2 to overestimate the dispersion contribution to the correlation energy.[56]

Comparison of adsorption energies calculated by DFT functionals with the reference CCSD(T) data showed that only functionals incorporating non-local dispersive electron correlation effects provided reasonable results. Adsorption energies ΔE calculated by the widely used semi-local GGA functional PBE were positive (except for ethanol; see Figure 3d), although geometry optimizations with the PBE functional found minima corresponding to adsorbed states of the molecules. In this case, slightly negative interaction energies ΔE_{int} (between −0.4 and −3.2 kcal/mol) were counterbalanced by positive deformation energies. Adsorption energies predicted by the B97D functional, which accounts for London dispersive forces by empirical corrections, were in close agreement with CCSD(T) values, with a ME of 2.4 kcal/mol. However, such empirical corrections are pairwise additive, which limits their use for larger systems.[57] The optB88-vdW functional, which includes a non-local core to account for non-local correlation effects (as well as many-body vdW energy), provided better adsorption energies compared to the CCSD(T) method (ME = 1.8 kcal/mol) and therefore was used for the simulations of molecules on graphene. It should be noted that vdW-DF[12]-based functionals have been shown to be highly sensitive to the exchange component, particularly in the case of metal−graphene interactions.[58,59] Hybrid meta-GGA M06-2X functional, which accounts for dispersion using a reparametrized exchange-correlation functional, gave the lowest ME of 0.9 kcal/mol with respect to the CCSD(T)/CBS estimate of adsorption energies.

For the sake of completeness, we also compared interaction energies ΔE_{int} (i.e., energies not including the deformation energies) obtained by the optB88-vdW, M06-2X, and SCS-(MI)-MP2 methods (i.e., the best-performing functionals and wave function-based method) against those calculated from the

dx.doi.org/10.1021/ja403162r | J. Am. Chem. Soc. 2013, 135, 6372−6377

Table 3. Adsorption Energies ΔE (and Enthalpies ΔH, see text for details, both in kcal/mol) Obtained by Quenching AIMD Simulations (ΔE^{AIMD} and ΔH^{AIMD}), Averaging Energies Obtained in AIMD Simulations ($\Delta\langle E^{AIMD}\rangle$ and $\Delta\langle H^{AIMD}\rangle$), and from Force Field Simulations ($\Delta\langle H^{FF}\rangle$); Experimental Adsorption Enthalpies ΔH_{ads} Are Also Listed

compound	$\Delta\langle H^{FF}\rangle$	ΔE^{AIMD}	$\Delta\langle E^{AIMD}\rangle$	ΔH^{AIMD}	$\Delta\langle H^{AIMD}\rangle$	ΔH_{ads}
acetone	−6.6	−9.3	−8.3	−7.8	−7.9	−8.2 ± 0.3
acetonitrile	−5.0	−8.0	−6.9	−6.6	−6.8	−7.6 ± 0.3
dichloromethane	−6.3	−7.2	−5.8	−5.7	−5.8	−5.9 ± 0.5
ethanol	−5.0	−7.9	−6.9	−6.2	−6.4	−7.3 ± 0.7
ethyl acetate	−9.4	−13.1	−11.5	−11.5	−11.2	−11.5 ± 0.2
hexane	−10.2					−12.2 ± 0.2
toluene	−10.5	−15.1	−12.9	−14.0	−12.7	−13.5 ± 0.3

benchmark CCSD(T) method (Table 2). The MEs (0.6, 0.8, and 0.4 kcal/mol for optB88-vdW, M06-2X, and SCS(MI)-MP2, respectively) were lower than the thermochemical accuracy (1 kcal/mol) usually required for such types of calculations. Owing to the high quality (low ME of the energy) and reasonable computational demands, we recommend all three methods for calculations of the interaction energies of organic molecules to coronene. Full data sets of the adsorption and interaction energies of molecules on coronene are provided in Tables S3 and S4.

Computations on Graphene. The adsorption enthalpies of molecules on graphene were initially calculated using the empirical OPLS-AA force field. The resulting enthalpies $\Delta\langle H^{FF}\rangle$ (Table 3) correlated to the experimental data with a correlation coefficient of r = 0.93. Compared to the experimental data, the force field energies were underestimated by an average ME of 1.9 kcal/mol. This might be due to the neglect of polarization energy in the pairwise additive force fields[60] and other limitations of classical force fields.[57] Nevertheless, the OPLS-AA force field was able to recognize weakly and strongly bound molecules, and thus may be suitable for semi-quantitative estimates of the interaction energies of large molecules with graphene.

Based on the above-mentioned results, we applied the optB88-vdW functional to obtain the adsorption enthalpies of molecules on graphene at a quantum mechanical level by AIMD. The starting configurations were adopted as the geometries obtained from the molecule−coronene system optimizations (Figure 2). All molecules remained bound to the graphene surface during the AIMD simulations, with the average surface−molecule distance corresponding to physisorption. It should be noted that, in test AIMD with the standard PBE functional,[49] the molecules spontaneously detached from the graphene surface, which underlines the importance of non-local dispersive correlations. Adsorption energies obtained by quenching low-energy AIMD configurations (ΔE^{AIMD}) and time-averaged energies from AIMD runs ($\Delta\langle E^{AIMD}\rangle$) are reported in Table 3. The time-averaged energies intrinsically included a contribution from thermal vibrations ($\Delta\Delta E_T$) to the internal energy, which slightly increased the adsorption energy ($\Delta E^{AIMD} < \Delta\langle E^{AIMD}\rangle$; Table 3). However, the adsorbed molecules did not alter the electronic structure of graphene, as shown by the band structure (Supporting Information, Figure S9).

The close agreement between experimental and calculated values of the adsorption enthalpies ΔH^{AIMD} and $\Delta\langle H^{AIMD}\rangle$, obtained from ΔE^{AIMD} and $\Delta\langle E^{AIMD}\rangle$, respectively, by adding appropriate corrections (see Methods section for details), indicates that thermal vibrations were well described, even by using the harmonic approximation on the coronene model. Theoretical enthalpies of adsorption followed the same order as the measured adsorption enthalpies, with the strongest binding being that of toluene and the weakest binding for dichloromethane. Moreover, the absolute values of the calculated adsorption enthalpies were in excellent agreement with the experimental values (r = 0.99, ME = 0.4 kcal/mol for $\Delta\langle H^{AIMD}\rangle$ and r = 0.99, ME = 0.5 kcal/mol for ΔH^{AIMD}). This agreement shows that modern DFT functionals that include non-local dispersive interactions can reliably treat even difficult systems, such as a molecule adsorbed on a two-dimensional graphene sheet.

CONCLUSIONS

Inverse gas chromatography measurements provided experimental values for the adsorption enthalpies of seven organic molecules on graphene flakes with an error less than 0.7 kcal/mol (ME = 0.4 kcal/mol). Molecule−coronene systems were modeled to calculate the strength and nature of the interaction together with the effect of zero-point energy, thermal vibration, and enthalpy corrections to the adsorption enthalpy. SAPT calculations showed that all the considered complexes were predominantly stabilized by dispersion, which contributes more than 60% to the attractive energy, even in polar complexes. The change in zero-point energy upon adsorption was similar for each molecule and led to an increase of the adsorption energy by about 0.8−1.3 kcal/mol. Thermal vibrations further increased the energy by 0.9−1.6 kcal/mol. Thermal correction to the enthalpy had an opposite effect, decreasing the energy by ∼ −0.7 kcal/mol, equivalent to $-RT$ for an ideal gas. As these contributions were similar (and rather small) for all the considered molecules, we concluded that the adsorption enthalpy is mainly controlled by the interaction energy. *Ab initio* MD simulations of molecules on graphene were performed using the optB88-vdW functional. We found that the order and absolute values of the theoretical adsorption enthalpies were in excellent agreement with the experimental values, indicating that the non-local electron correlation is crucial for proper description of the adsorption to graphene at the DFT level.

ASSOCIATED CONTENT

Supporting Information

Figure S1, SEM images and EDS spectra of graphene flakes; Figures S2−S8, measured slopes of $\ln P$ against $1/T$ for each molecule; Figure S9, band structures; details on energy calculations; Table S1, SAPT components; Table S2, adsorption enthalpy contributions; Tables S3 and S4, adsorption and interaction energies on coronene; and Table S5, adsorption geometries of molecules on coronene. This

dx.doi.org/10.1021/ja403162r | J. Am. Chem. Soc. 2013, 135, 6372−6377

material is available free of charge via the Internet at http://pubs.acs.org.

AUTHOR INFORMATION

Corresponding Author

michal.otyepka@upol.cz

Author Contributions

‡P.L. and F.K. contributed equally.

Notes

The authors declare no competing financial interest.

ACKNOWLEDGMENTS

This work was supported by the Grant Agency of the Czech Republic (P208/12/G016 and P208/10/1742), the Operational Program Research and Development for Innovations−European Regional Development Fund (CZ.1.05/2.1.00/03.0058), the Operational Program Education for Competitiveness−European Social Fund (CZ.1.07/2.3.00/20.0017), and a student project of Palacký University (PrF_2013_028).

REFERENCES

(1) Novoselov, K. S.; Geim, A. K.; Morozov, S. V.; Jiang, D.; Zhang, Y.; Dubonos, S. V.; Grigorieva, I. V.; Firsov, A. A. *Science* **2004**, *306*, 666.

(2) Geim, A. K.; Novoselov, K. S. *Nat. Mater.* **2007**, *6*, 183.

(3) Novoselov, K. S.; Falko, V. I.; Colombo, L.; Gellert, P. R.; Schwab, M. G.; Kim, K. *Nature* **2012**, *490*, 192.

(4) Georgakilas, V.; Otyepka, M.; Bourlinos, A. B.; Chandra, V.; Kim, N.; Kemp, K. C.; Hobza, P.; Zboril, R.; Kim, K. S. *Chem. Rev.* **2012**, *112*, 6156.

(5) Schedin, F.; Geim, A. K.; Morozov, S. V.; Hill, E. W.; Blake, P.; Katsnelson, M. I.; Novoselov, K. S. *Nat. Mater.* **2007**, *6*, 652.

(6) Myung, S.; Yin, P. T.; Kim, C.; Park, J.; Solanki, A.; Reyes, P. I.; Lu, Y. C.; Kim, K. S.; Lee, K. B. *Adv. Mater.* **2012**, *24*, 6081.

(7) Hohenberg, P.; Kohn, W. *Phys. Rev. B* **1964**, *136*, B864.

(8) Kohn, W.; Sham, L. J. *Phys. Rev.* **1965**, *140*, 1133.

(9) Burke, K. *J. Chem. Phys.* **2012**, *136*, 150901.

(10) Cohen, A. J.; Mori-Sanchez, P.; Yang, W. T. *Chem. Rev.* **2012**, *112*, 289.

(11) Grimme, S. *Wires Comput. Mol. Sci.* **2011**, *1*, 211.

(12) Dion, M.; Rydberg, H.; Schroder, E.; Langreth, D. C.; Lundqvist, B. I. *Phys. Rev. Lett.* **2004**, *92*, 246401.

(13) Eshuis, H.; Bates, J. E.; Furche, F. *Theor. Chem. Acc.* **2012**, *131*, 1084.

(14) Ren, X. G.; Rinke, P.; Joas, C.; Scheffler, M. *J. Mater. Sci.* **2012**, *47*, 7447.

(15) Papirer, E.; Brendle, E.; Ozil, F.; Balard, H. *Carbon* **1999**, *37*, 1265.

(16) Balard, H.; Maafa, D.; Santini, A.; Donnet, J. B. *J. Chromatogr. A* **2008**, *1198−1199*, 173.

(17) Menzel, R.; Bismarck, A.; Shaffer, M. S. P. *Carbon* **2012**, *50*, 3416.

(18) Díaz, E.; Ordóñez, S.; Vega, A.; Coca, J. *J. Chromatogr. A* **2004**, *1049*, 139.

(19) Klimes, J.; Bowler, D. R.; Michaelides, A. *Phys. Rev. B* **2011**, *83*, 195313.

(20) Antony, J.; Grimme, S. *Phys. Chem. Chem. Phys.* **2008**, *10*, 2722.

(21) Umadevi, D.; Sastry, G. N. *J. Phys. Chem. Lett.* **2011**, *2*, 1572.

(22) Min, S. K.; Kim, W. Y.; Cho, Y.; Kim, K. S. *Nature Nanotechnol.* **2011**, *6*, 162.

(23) Zhang, T.; Xue, Q.; Zhang, S.; Dong, M. *Nano Today* **2012**, *7*, 180.

(24) Janowski, T.; Pulay, P. *J. Am. Chem. Soc.* **2012**, *134*, 17520.

(25) Smith, D. G. A.; Patkowski, K. *J. Chem. Theory Comput.* **2013**, *9*, 370.

(26) Kysilka, J.; Rubes, M.; Grajciar, L.; Nachtigall, P.; Bludsky, O. *J. Phys. Chem. A* **2011**, *115*, 11387.

(27) Voloshina, E.; Usvyat, D.; Schutz, M.; Dedkov, Y.; Paulus, B. *Phys. Chem. Chem. Phys.* **2011**, *13*, 12041.

(28) Podeszwa, R. *J. Chem. Phys.* **2010**, *132*, 044704.

(29) Szalewicz, K. *Wires Comput. Mol. Sci.* **2012**, *2*, 254.

(30) Panzer, U.; Schreiber, H. P. *Macromolecules* **1992**, *25*, 3633.

(31) Conder, J. R.; Young, C. L. *Physicochemical measurement by gas chromatography*; Wiley: New York, 1979.

(32) Ahlrichs, R.; Bar, M.; Haser, M.; Horn, H.; Kolmel, C. *Chem. Phys. Lett.* **1989**, *162*, 165.

(33) Werner, H. J.; Knowles, P. J.; Knizia, G.; Manby, F. R.; Schutz, M. *MOLPRO*, version 2012.1, a package of ab initio programs, 2012; http://www.molpro.net.

(34) Halkier, A.; Helgaker, T.; Jørgensen, P.; Klopper, W.; Koch, H.; Olsen, J.; Wilson, A. K. *Chem. Phys. Lett.* **1998**, *286*, 243.

(35) Jurecka, P.; Hobza, P. *J. Am. Chem. Soc.* **2003**, *125*, 15608.

(36) Riley, K. E.; Rezac, J.; Hobza, P. *Phys. Chem. Chem. Phys.* **2011**, *13*, 21121.

(37) Distasio, R. A.; Head-Gordon, M. *Mol. Phys.* **2007**, *105*, 1073.

(38) Boys, S. F.; Bernardi, F. *Mol. Phys.* **1970**, *19*, 553.

(39) Zhao, Y.; Truhlar, D. *Theor. Chem. Acc.* **2008**, *120*, 215.

(40) Grimme, S. *J. Comput. Chem.* **2006**, *27*, 1787.

(41) Frisch, M. J.; Trucks, G. W.; Schlegel, H. B.; Scuseria, G. E.; Robb, M. A.; Cheeseman, J. R.; Scalmani, G.; Barone, V.; Mennucci, B.; Petersson, G. A.; Nakatsuji, H.; Caricato, M.; Li, X.; Hratchian, H. P.; Izmaylov, A. F.; Bloino, J.; Zheng, G.; Sonnenberg, J. L.; Hada, M.; Ehara, M.; Toyota, K.; Fukuda, R.; Hasegawa, J.; Ishida, M.; Nakajima, T.; Honda, Y.; Kitao, O.; Nakai, H.; Vreven, T.; Montgomery, J. A.; Peralta, J. E.; Ogliaro, F.; Bearpark, M.; Heyd, J. J.; Brothers, E.; Kudin, K. N.; Staroverov, V. N.; Kobayashi, R.; Normand, J.; Raghavachari, K.; Rendell, A.; Burant, J. C.; Iyengar, S. S.; Tomasi, J.; Cossi, M.; Rega, N.; Millam, J. M.; Klene, M.; Knox, J. E.; Cross, J. B.; Bakken, V.; Adamo, C.; Jaramillo, J.; Gomperts, R.; Stratmann, R. E.; Yazyev, O.; Austin, A. J.; Cammi, R.; Pomelli, C.; Ochterski, J. W.; Martin, R. L.; Morokuma, K.; Zakrzewski, V. G.; Voth, G. A.; Salvador, P.; Dannenberg, J. J.; Dapprich, S.; Daniels, A. D.; Farkas; Foresman, J. B.; Ortiz, J. V.; Cioslowski, J.; Fox, D. J. *Gaussian 09*, Revision A.02; Wallingford CT, 2009.

(42) Hesselmann, A.; Jansen, G. *Chem. Phys. Lett.* **2002**, *362*, 319.

(43) Hesselmann, A.; Jansen, G. *Chem. Phys. Lett.* **2002**, *357*, 464.

(44) Hesselmann, A.; Jansen, G. *Chem. Phys. Lett.* **2003**, *367*, 778.

(45) Hesselmann, A.; Jansen, G.; Schutz, M. *J. Chem. Phys.* **2005**, *122*, 014103.

(46) Della Sala, F.; Gorling, A. *J. Chem. Phys.* **2001**, *115*, 5718.

(47) Gruning, M.; Gritsenko, O. V.; van Gisbergen, S. J. A.; Baerends, E. J. *J. Chem. Phys.* **2001**, *114*, 652.

(48) Adamo, C.; Barone, V. *J. Chem. Phys.* **1999**, *110*, 6158.

(49) Perdew, J. P.; Burke, K.; Ernzerhof, M. *Phys. Rev. Lett.* **1997**, *78*, 1396.

(50) Blochl, P. E. *Phys. Rev. B* **1994**, *50*, 17953.

(51) Kresse, G.; Joubert, D. *Phys. Rev. B* **1999**, *59*, 1758.

(52) Jorgensen, W. L.; Tirado-Rives, J. *Proc. Natl. Acad. Sci. U.S.A.* **2005**, *102*, 6665.

(53) Caleman, C.; van Maaren, P. J.; Hong, M. Y.; Hub, J. S.; Costa, L. T.; van der Spoel, D. *J. Chem. Theory Comput.* **2012**, *8*, 61.

(54) van der Spoel, D.; van Maaren, P. J.; Caleman, C. *Bioinformatics* **2012**, *28*, 752.

(55) Cheng, A.; Steele, W. A. *J. Chem. Phys.* **1990**, *92*, 3858.

(56) Riley, K. E.; Pitonak, M.; Jurecka, P.; Hobza, P. *Chem. Rev.* **2010**, *110*, 5023.

(57) DiStasio, R. A.; von Lilienfeld, O. A.; Tkatchenko, A. *Proc. Natl. Acad. Sci. U.S.A.* **2012**, *109*, 14791.

(58) Granatier, J.; Lazar, P.; Otyepka, M.; Hobza, P. *J. Chem. Theory Comput.* **2011**, *7*, 3743.

(59) Granatier, J.; Lazar, P.; Prucek, R.; Safarova, K.; Zboril, R.; Otyepka, M.; Hobza, P. *J. Phys. Chem. C* **2012**, *116*, 14151.

(60) Zgarbova, M.; Otyepka, M.; Sponer, J.; Hobza, P.; Jurecka, P. *Phys. Chem. Chem. Phys.* **2010**, *12*, 10476.